Lower Locus Coeruleus MRI intensity in patients with late-life major depression

Andrés Guinea-Izquierdo [Equal first author, 1, 2] , **Mónica Giménez** [Equal first author, 2] , **Ignacio Martínez-Zalacaín** [1, 2] , **Inés del Cerro** [1, 2, 3] , **Pol Canal-Noguer** [4, 5, 6] , **Gerard Blasco** [7] , **Jordi Gascón** [8] , **Ramon Reñé** [8] , **Inmaculada Rico** [8] , **Angels Camins** [7] , **Carlos Aguilera** [7] , **Mikel Urretavizcaya** [1, 2, 3] , **Isidre Ferrer** [9, 10, 11] , **José Manuel Menchón** [1, 2, 3] , **Virginia Soria** [Corresp., 1, 2, 3] , **Carles Soriano-Mas** [Corresp. 2, 3, 12]

1 Department of Clinical Sciences / School of Medicine, University of Barcelona, Barcelona, Spain

2 Department of Psychiatry / Bellvitge University Hospital, Bellvitge Biomedical Research Institute (IDIBELL), Hospitalet de Llobregat (Barcelona), Spain

3 Network Center for Biomedical Research on Mental Health (CIBERSAM), Madrid, Spain

4 B2SLab / Departament d'Enginyeria de Sistemes, Automàtica i Informàtica Industrial, Universitat Politècnica de Catalunya, Barcelona, Spain

5 Networking Biomedical Research Centre in the subject area of Bioengineering, Biomaterials and Nanomedicine (CIBER-BBN), Madrid, Spain

6 Institut de Recerca Pediàtrica, Hospital Sant Joan de Déu, Esplugues de Llobregat (Barcelona), Spain

7 Imaging Diagnostic Institute (IDI), Bellvitge University Hospital, Hospitalet de Llobregat (Barcelona), Spain

8 Dementia Diagnostic and Treatment Unit / Department of Neurology, Bellvitge University Hospital, Hospitalet de Llobregat (Barcelona), Spain

9 Department of Pathology and Experimental Therapeutics / Institute of Neurosciences, University of Barcelona, Hospitalet de Llobregat (Barcelona), Spain

10 Department of Pathologic Anatomy / Bellvitge University Hospital, Bellvitge Biomedical Research Institute-IDIBELL, Hospitalet de Llobregat (Barcelona), Spain

11 Network Center for Biomedical Research on Neurodegenerative diseases (CIBERNED), Madrid, Spain

12 Department of Psychobiology and Methodology in Health Sciences, Universitat Autónoma de Barcelona, Bellaterra (Barcelona), Spain

Corresponding Authors: Virginia Soria, Carles Soriano-Mas
Email address: vsoria@bellvitgehospital.cat, csoriano@idibell.cat

Background. The locus coeruleus (LC) is the major noradrenergic source in the central nervous system. Structural alterations in the LC contribute to the pathophysiology of different neuropsychiatric disorders, which may increase to a variable extent the likelihood of developing neurodegenerative conditions. The characterization of such alterations may therefore help to predict progression to neurodegenerative disorders. Despite the LC cannot be visualized with conventional magnetic resonance imaging (MRI), specific MRI sequences have been developed to infer its structural integrity. **Methods.** We quantified LC signal Contrast Ratios (LCCRs) in late-life major depressive disorder (MDD) (n=37, 9 with comorbid aMCI), amnestic Mild Cognitive Impairment (aMCI) (n=21, without comorbid MDD), and healthy controls (HCs) (n=31), and also assessed the putative modulatory effects of comorbidities and other clinical variables. **Results.** LCCRs were lower in MDD compared to aMCI and HCs. While no effects of aMCI comorbidity were observed, lower LCCRs were specifically observed in patients taking serotonin/norepinephrine reuptake inhibitors (SNRIs). **Conclusion.** Our results do not support the hypothesis that lower LCCRs characterize the different clinical groups that may eventually develop a neurodegenerative

disorder. Conversely, our results were specifically observed in patients with late-life MDD taking SNRIs. Further research with larger samples is warranted to ascertain whether medication or particular clinical features of patients taking SNRIs are associated with changes in LC neurons.

1 --Title Page--

3 Lower Locus Coeruleus MRI intensity in patients with
4 late-life major depression

6 Andrés Guinea-Izquierdo, MSc[1,2*], Mónica Giménez, PhD[1*], Ignacio Martínez-Zalacaín, MSc[1,2],
7 Inés del Cerro, MSc[1,2,3], Pol Canal-Noguer, MSc[4,5,6], Gerard Blasco, PhD[7], Jordi Gascón, MD[8],
8 Ramón Reñé, MD, PhD[8], Inmaculada Rico[8], Àngels Camins MD[7], Carlos Aguilera MD PhD[7],
9 Mikel Urretavizcaya, MD PhD[1,2,3], Isidre Ferrer, MD PhD[9,10,11], José M Menchón, MD PhD[1,2,3],
10 Virginia Soria, MD PhD[1,2,3#], Carles Soriano-Mas, PhD[1,3,12#]

12 *These authors contributed equally to the work
13 # Shared corresponding author

15 [1] Bellvitge Biomedical Research Institute-IDIBELL, Department of Psychiatry, Bellvitge
16 University Hospital, L'Hospitalet de Llobregat, Barcelona, Spain
17 [2] Department of Clinical Sciences, School of Medicine, University of Barcelona, Barcelona,
18 Spain
19 [3] Network Center for Biomedical Research on Mental Health (CIBERSAM), Carlos III Health
20 Institute (ISCIII), Madrid, Spain
21 [4] B2SLab, Departament d'Enginyeria de Sistemes, Automàtica i Informàtica Industrial,
22 Universitat Politècnica de Catalunya, Barcelona, Spain
23 [5] Networking Biomedical Research Centre in the subject area of Bioengineering, Biomaterials
24 and Nanomedicine (CIBER-BBN), Madrid, Spain
25 [6]   Institut de Recerca Pediàtrica, Hospital Sant Joan de Déu, Esplugues de Llobregat, Spain
26 [7]   Imaging Diagnostic Institute (IDI), Bellvitge University Hospital, Hospitalet de Llobregat,
27 Barcelona, Spain
28 [8] Dementia Diagnostic and Treatment Unit, Department of Neurology, Bellvitge University
29 Hospital, Hospitalet de Llobregat, Barcelona, Spain
30 [9] Department of Pathology and Experimental Therapeutics, Institute of Neurosciences,
31 University of Barcelona, Hospitalet de Llobregat, Barcelona, Spain
32 [10]   Bellvitge Biomedical Research Institute-IDIBELL, Department of Pathologic Anatomy,
33 Bellvitge University Hospital, Hospitalet de Llobregat, Barcelona, Spain
34 [11]   Network Center for Biomedical Research on Neurodegenerative diseases (CIBERNED),
35 Hospitalet de Llobregat, Barcelona, Spain
36 [12]   Department of Psychobiology and Methodology in Health Sciences, Universitat Autònoma
37 de Barcelona, Bellaterra, Barcelona, Spain

38

39

40 **Corresponding Authors**

41

42   Carles Soriano-Mas

43

44   Department of Psychiatry, Bellvitge University Hospital, Bellvitge Biomedical Research
45   Institute-IDIBELL. Feixa Llarga s/n, 08907, L'Hospitalet de Llobregat, Barcelona, Spain
46   Email address: csoriano@idibell.cat

47

48   Virginia Soria

49

50   Department of Psychiatry, Bellvitge University Hospital, Bellvitge Biomedical Research
51   Institute-IDIBELL. Feixa Llarga s/n, 08907, L'Hospitalet de Llobregat, Barcelona, Spain.
52   Email address: vsoria @bellvitgehospital.cat

Abstract

Background. The locus coeruleus (LC) is the major noradrenergic source in the central nervous system. Structural alterations in the LC contribute to the pathophysiology of different neuropsychiatric disorders, which may increase to a variable extent the likelihood of developing neurodegenerative conditions. The characterization of such alterations may therefore help to predict progression to neurodegenerative disorders. Despite the LC cannot be visualized with conventional magnetic resonance imaging (MRI), specific MRI sequences have been developed to infer its structural integrity.

Methods. We quantified LC signal Contrast Ratios (LCCRs) in late-life major depressive disorder (MDD) (n=37, 9 with comorbid aMCI), amnestic Mild Cognitive Impairment (aMCI) (n=21, without comorbid MDD), and healthy controls (HCs) (n=31), and also assessed the putative modulatory effects of comorbidities and other clinical variables.

Results. LCCRs were lower in MDD compared to aMCI and HCs. While no effects of aMCI comorbidity were observed, lower LCCRs were specifically observed in patients taking serotonin/norepinephrine reuptake inhibitors (SNRIs).

Conclusion. Our results do not support the hypothesis that lower LCCRs characterize the different clinical groups that may eventually develop a neurodegenerative disorder. Conversely, our results were specifically observed in patients with late-life MDD taking SNRIs. Further research with larger samples is warranted to ascertain whether medication or particular clinical features of patients taking SNRIs are associated with changes in LC neurons.

Introduction

The Locus Coeruleus (LC) is a small pontine nucleus with the largest group of noradrenergic (NA) neurons in the central nervous system (CNS) (Berridge & Waterhouse, 2003; Dahlstroem & Fuxe, 1964). Its ascending and descending projections modulate neuronal activity in numerous targets throughout the CNS (Loughlin, Foote & Fallon, 1982; Loughlin, Foote & Grzanna, 1986; Loughlin, Foote & Bloom, 1986; Samuels & Szabadi, 2008). Different studies suggest that alterations in the LC, and, hence, in its projection network, may critically contribute to the onset as well as to the course and symptom profile of a range of neurological and psychiatric disorders (Betts et al., 2019; Charney, 1998; Delgado & Moreno, 2000; Gannon et al., 2015; Leonard, 1997). Specifically, the LC has been suggested to be one of the initial sites of appearance of pathologically altered tau aggregates in preclinical stages of Alzheimer's disease (AD) (Braak et al., 2011; Braak and Del Tredici, 2015; Zarow et al., 2003), leading to compensatory increases in α2A adrenergic receptor levels in regions receiving noradrenergic input (Andrés-Benito et al., 2017). Moreover, there is evidence that loss of noradrenergic input exacerbates AD progression (Marien et al., 2004; Heneka et al., 2006; Grudzien et al., 2007).

One of the major limitations to investigate the role of the LC in brain disorders with in-vivo non-invasive techniques is that the LC is difficult to visualize with conventional magnetic resonance imaging (MRI) techniques. However, Sasaki et al. (2006) identified the LC in vivo as two bilateral hyperintensities adjacent to the floor of the fourth ventricle adapting the parameters of a traditional 2D T1-weighted fast spin echo sequence (for instance, using a higher number of averages and a high in-plane resolution with a large slice thickness). The molecular underpinnings of such hyperintense signal are still unknown (Betts et al., 2019), although it was originally thought to be related with the accumulation of neuromelanin in LC neurons.

Neuromelanin is a dark polymer pigment formed as a byproduct of catecholamine metabolism, and it can be found in the LC and substantia nigra pars compacta. The function of this macromolecule is not entirely known, but it has been shown that neuromelanin accumulates throughout life in noradrenergic LC neurons, binding to metals such as iron and copper (Enochs et al., 1989, 1997; Trujillo et al., 2017). Due to its ability to chelate metals, neuromelanin could be acting as a paramagnetic agent (Tosk et al., 1992), and perhaps neuromelanin could be a paramagnetic agent itself (Shima et al., 1997). These properties initially led some authors to hypothesize that neuromelanin could be causing the T1 shortening effects generating the LC contrast in fast spin echo T1 sequences (Sasaki et al., 2006).

Moreover, using MRI and post mortem histology, Keren et al. (2015) showed that T1-weighted LC hyperintensities co-localized with LC neurons with high neuromelanin concentration. Nevertheless, more recent research suggested that it is unlikely that LC hyperintensities are reflecting neuromelanin accumulation, but rather water content or general neuronal density

121 (Watanabe et al., 2019). In this sense, throughout the manuscript, we will avoid using the term
122 neuromelanin-sensitive MRI, although it may be concluded from the literature that LC MRI
123 contrast ratios (LCCRs) seem to be a valid approximation to infer structural integrity of the LC
124 (Betts et al., 2019).
125
126 There have been different reports of an overall lower LC signal in different neuropsychiatric
127 conditions, such as major depressive disorder (MDD) (Sasaki et al., 2010; Shibata et al., 2008),
128 schizophrenia (Shibata et al., 2008), amnestic mild cognitive impairment (aMCI) (Takahashi et
129 al., 2015), and Alzheimer's or Parkinson's disease (Sasaki et al., 2006; Isaias et al., 2016;
130 Matsuura et al., 2013; Miyoshi et al., 2013; Mukai et al., 2013; Ohtsuka et al., 2014), among
131 others (for a review see Liu et al., 2017). It is not clear, however, to what extent such alterations
132 show diagnostic specificity, which might be useful for clinical purposes (e.g., differential
133 diagnosis, treatment selection, or prediction of clinical course). This could be important for
134 disorders with partially overlapping clinical manifestations, such as late-life MDD and aMCI,
135 two conditions typically appearing between the seventh and the eighth decades of life (Panza et
136 al., 2010; Steffens, 2012).
137
138 People suffering from late-life MDD or aMCI have an increased risk for the later development of
139 AD. Nevertheless, while aMCI is a common prodromal stage of AD, with a progression rate to
140 AD estimated between 6% to 25% per year (Petersen, 2001) (for a review see Hermida et al.,
141 2012), late-life MDD is not that robustly associated with dementia onset, and results have been
142 more heterogeneous. Overall, research suggests that people suffering from late-life MDD have
143 an approximately twofold increased risk of developing AD (Byers & Yaffe, 2011), although it is
144 not clear whether depression is only a risk factor or may be considered a prodromal symptom of
145 dementia (Byers & Yaffe, 2011). Interestingly, moreover, co-occurrence of aMCI and depression
146 seems to increase even more the probability to develop to AD, suggesting that both conditions
147 have an additive or synergic effect (Modrego & Ferrandez, 2004; Gabryelewicz et al., 2007). In
148 this context, it is not clear whether LC MRI intensity discriminates between these disorders and
149 their comorbidity, and, therefore, to what extent this measurement could contribute to identify
150 subjects at a higher risk of developing a neurodegenerative disorder.
151
152 In this study, we aimed at comparing LC MRI intensity between patients with late-life MDD and
153 individuals with aMCI, which, for reference purposes, were also compared to a group of healthy
154 controls (HCs). Moreover, as a secondary aim, we specifically assessed a group of individuals
155 presenting comorbidity between the two diagnoses, and evaluated the modulatory effect on our
156 findings of medication and other clinical variables. According to previous literature, we
157 hypothesized that LC MRI intensity will discriminate between the clinical groups and HCs, and
158 also across patients with late-life MDD, aMCI and a comorbid presentation of both disorders.

Materials & Methods

Participants

The sample consisted of 89 individuals between 60 and 76 years of age. These were divided into three groups: 37 patients with a primary diagnosis of late-life MDD (11 males, mean age [standard deviation, SD]: 68 [4.1] years), 21 subjects with aMCI (9 males, mean age: 71.5 [2.7] years), and 31 HCs from the same geographical area (11 males, mean age [SD]: 67.7 [4.1] years. Subjects from the clinical groups were consecutively recruited from the Psychiatry and Neurology Departments of Bellvitge University Hospital (Barcelona, Spain), and HCs through advertisements and word-of-mouth. All participants were interviewed with the Mini-International Neuropsychiatric Interview (MINI) (Sheehan et al., 1998). MDD diagnoses were established by two experienced psychiatrists (VS and MU) according to DSM-IV-TR criteria, and disorder severity was estimated with the Hamilton Depression Rating Scale (HDRS) (Hamilton, 1960) and the Geriatric Depression Scale (GDS) (Sheikh & Yesavage, 1986; Yesavage et al., 1982), which were, however, not used for diagnostic purposes. Amnestic MCI diagnoses were based on a syndromic categorical cognitive staging approach rather than on the use of biomarkers (Jack et al., 2018). Diagnosis was established by consensus of two experienced neurologists (JG and RR) and one neuropsychologist (IR) following Petersen criteria (Petersen, 2004), including: 1) complaints of memory loss confirmed by informants, 2) objective long-term memory impairments (scores 1.5 SD below mean age and education adjusted normative values in the delayed recall test from the Wechsler Memory Scale III (WMS-III) (Wechsler, 2004) and the brief neuropsychological battery NBACE (Alegret et al., 2012), 3) preserved general cognitive functioning (i.e., scores higher than 23 for literate people and higher than 18 for illiterates in the Spanish version of the Mini Mental State Examination (MMSE) (Folstein & Folstein, 1975), and 4) intact or mildly impaired daily living abilities (Clinical Dementia Rating (CDR) (Morris,1993) scores of 0.5). All participants were also administered the Vocabulary subtest of the Wechsler Adult Intelligence Scale, Third Edition (WAIS-III) (Wechsler, 1999), to estimate the premorbid intelligence quotient (IQ) (García-Lorenzo et al., 2013). Importantly, aMCI participants did not present past or current comorbidity with MDD, while nine out of the 37 patients with MDD presented a comorbid aMCI diagnosis. In all cases, medication was not changed and was kept at stable doses for at least one month before MRI acquisition. Fourteen out of 21 aMCI subjects were taking antidepressants for conditions other than MDD, such as impaired psychosocial adjustment, insomnia or headache. Table 1 summarizes the sociodemographic and clinical characteristics of the study sample, while information about antidepressant medication is provided in Table 2.

Exclusion criteria for the study participants included: 1) ages <60 or >76 years, 2) past or current diagnosis of other major psychiatric disorders including substance abuse or dependence (except nicotine), 3) intellectual disability/neurodevelopmental disorders, 4) neurological disorders, 5)

199   Hachinski Ischemic Score >5 to exclude individuals with a high probability of vascular-derived
200   cognitive deficits, 6) presence of dementia according to the DSM-IV-TR criteria and/or a CDR
201   score>1, 7) severe medical conditions, 8) electroconvulsive therapy in the previous year, 9)
202   conditions preventing neuropsychological assessment or MRI procedures (e.g., blindness,
203   deafness, claustrophobia, pacemakers or cochlear implants), and 10) gross abnormalities in the
204   MRI scan. We also evaluated the presence of vascular pathology in our brain region of interest
205   (pons), finding no significant alterations preventing accurate image processing and analysis.
206
207   The study was approved by The Clinical Research Ethics Committee (CEIC) of Bellvitge
208   University Hospital (reference PR156/15, February 17th 2016) and performed in accordance
209   with the ethical standards laid down in the 1964 Declaration of Helsinki and its later
210   amendments (revised in 2013). All participants gave written informed consent to participate in
211   the study.
212
213
214   **MRI scanning protocol**
215
216   All scans were performed in a 3T Philips Ingenia Scanner (Koninklijke Philips N.V.,
217   Netherlands), using a 32-channel head coil. Following previous reports (Sasaki et al., 2006), we
218   obtained a modified T1-weighted fast spin-echo sequence of the brainstem for LC visualization
219   (see examples of individual participants in Supplementary Figure S1). Acquisition parameters
220   were: TR 600 ms, TE 15 ms, 15 slices; 2.5 mm slice thickness, 0 mm gap, matrix size 404x250,
221   FOV 170x170 mm^2, acquisition voxel size 0.42x0.68x2.5 mm^3, reconstructed voxel size
222   0.39x0.39x2.5 mm^3, FA 90^0, 6 NEX (online averaging), and a total scan time of 15 minutes. The
223   sections were acquired in the oblique axial direction perpendicular to the floor of the fourth
224   ventricle, covering from the posterior commissure to the inferior border of the pons. Axial T1-
225   weighted turbo-gradient-echo high-resolution whole-brain anatomical images (233 slices,
226   TR=10.46 ms, TE=4.79 ms, flip angle= 8°, FOV= 240 x 240, 0.75 x 0.75mm isotropic voxels)
227   were additionally obtained for pre-processing purposes and to discard gross structural pathology.
228   Finally, we also obtained a 2D FLAIR sequence in the axial plane (38 slices, TR=10000 ms,
229   TE=140 ms, TI=2700 ms, FOV= 230 x 186, 0.8 x 1 x 3 mm voxels, 0.6 mm gap) to assess
230   vascular pathology and other potential radiological abnormalities. Throughout the acquisition
231   protocol, we used foam pads and made sure that patients' head was comfortably placed within
232   the head coil to avoid excessive movement.
233
234
235   **Localization and quantification of the LC**
236
237   To quantify LC MRI intensity, we used a semi-automated "in-house" algorithm. We focused our
238   analysis on the region of the dorsal pons. Specifically, our approach was based on previous
239   studies (García-Lorenzo et al, 2013) and consisted of two main steps:

240   *A): Delineation of regions of interest (ROIs):* We defined four rectangular ROIs onto the
241   Montreal Neurological Institute 152 [MNI 152] template (0.5mm isotropic resolution) using the
242   Statistical Parametric Mapping (SPM 12) software (http://www.fil.ion.ucl.ac.uk/spm/).
243   Specifically, two of these ROIs were symmetrically located in the left and right areas of the
244   dorsal pons where the LC is expected to be found, adjacent to the floor of the fourth ventricle
245   and extending to the level of the inferior colliculi. Importantly, we explicitly avoided including
246   in these ROIs other hyperintense regions, such as the substantia nigra, to ensure that the LC was
247   the highest signal intensity. The other two ROIs covered the mid portions of the adjacent left and
248   right pontine tegmentum (again, avoiding the inclusion of the substantia nigra), and were used as
249   a reference to standardize LC intensity values (see below). These ROIs, drawn in normalized
250   MNI space, were then denormalized to the native space of each participant. However, due to the
251   small size of the locus coeruleus and the anisotropic voxel size of the images, the LC sensitive
252   sequence was not manipulated and was used as the target image, therefore avoiding interpolation
253   artifacts and preserving the original signal. Consequently, we first linearly coregistered, for each
254   participant and in native space, the whole-brain T1 image to the LC sensitive image. Next, the
255   tissue probability map (TPM) and the four ROIs in MNI space were coregistered (linear
256   coregistration) to the whole-brain T1 image from the previous step, and such individual whole-
257   brain T1 images were non-linearly normalized to the coregistered TPM, which generated a
258   deformation field. The inverse of the deformation field was calculated by using the deformation
259   function in SPM, taking the LC sensitive image as the image to base the inversion on. The four
260   ROIs were then non-linearly denormalized to each participant native space by applying the
261   inverse of the deformation fields with a 4th degree b-spline interpolation. Finally, these ROIs
262   were binarized using a trilinear interpolation and a cut-off value of 0.1 (using the ImCalc
263   function; i1>0.1) in order to better delimitate the ROI area to be extracted; then, each binarized
264   ROI was applied to the LC-sensitive image (ImCalc function; i1.*i2), which effectively removed
265   from these images all the information outside the ROIs. Therefore, the final output of the process
266   were 4 images for participant, in native space, corresponding to the projection of each ROI into
267   the LC-sensitive image. This approach is summarized in Supplementary Figure S2. Likewise,
268   Supplementary Figure S3 displays the accuracy of the coregistration between the LC, the
269   reference ROI and the brainstem structures in native space.
270
271   *B): Quantification of the LC signal with a growing algorithm.* This second step was implemented
272   using an in-house growing algorithm, programmed in MATLAB version 9.3 (R2017b) (The
273   MathWorks Inc, Natick, Massachusetts), which was applied to the final output images from step
274   A) that encompassed the LC region. Specifically, following García-Lorenzo et al. (2013), who
275   defined LC as "the area of 10-connected voxels with the brightest intensity", the current
276   algorithm searched throughout these images the 10 clusters of 10 contiguous voxels (face and/or
277   edge and/or vertex contiguity) with the highest intensity (highest mean intensity of the cluster)
278   (see Figure 1). These clusters were visually inspected for their anatomical correspondence with
279   the region of the LC. In case the cluster with highest intensity was deemed to be outside the LC

280   region, the second cluster was inspected, and so on. Finally, we obtained, for each participant,
281   the 10-voxels cluster of highest signal intensity within the LC region, as well as the mean
282   intensity value and peak coordinate for this cluster (S_{LC}). In agreement with our interest in
283   assessing the intensity of LC, this 10-voxels average represents a good estimation of mean LC
284   intensity and its presumed neural integrity (Liu et al., 2017). This is different from a volume
285   measure of the nucleus; also, we did not discriminate intensities across the different territories of
286   the LC (García-Lorenzo et al., 2013).
287
288   The mean signal intensity from the reference pontine tegmentum cluster was also obtained for
289   each participant (S_{REF}). This value was used to control for putative differences in global signal
290   intensity across participants. We used the following formula to calculate the LC contrast ratio
291   (CR) (Liu et al., 2017): $CR = (S_{LC} - S_{REF}) / S_{REF}$. This CR was calculated for each participant and
292   for both LC (left and right), obtaining two different CRs for each participant (CR_{Left} and CR_{Right}
293     $_{Right}$). However, as we did not expect interhemispheric differences, and in order to simplify
294   statistical analyses, we averaged left and right CRs using the following formula: *average* LCCR=
295     $(CR_{Left} + CR_{Right}) / 2$. The *average* LCCR was the final variable used in the statistical analysis.
296
297
298   **Statistical analysis**
299
300   Differences in demographical and clinical features were contrasted across the three study groups
301   with the Kruskal-Wallis test for continuous variables and the Chi-Square test for categorical
302   variables. Differences in *average* LCCR were also assessed across the study groups using the
303   Kruskal-Wallis test. Having in mind that LC MRI contrast ratios interact with age (Liu et al.,
304   2019) and that structural and functional differences between men and women have been found in
305   this region (Bangasser et al, 2016; Mulvey et al, 2018), *average* LCCR comparisons were
306   controlled for age and sex. For this, we created a new variable (*standardized residual of average*
307   LCCR*, sra*LCCR) extracting the effect of both variables, as non-parametrical tests do not allow
308   nuisance covariates. When the Kruskal-Wallis test showed significant differences across the
309   three groups, pairwise comparisons were assessed using the Mann–Whitney's U test. Moreover,
310   we used Spearman's Rho (r_s) correlations to evaluate the possible associations between *sraLCCR*
311   and different clinical features (i.e., dose and duration of treatments, MMSE).
312
313   Finally, we analyzed the modulatory effect of treatment (e.g., treatment type, duration or dose)
314   on *sra*LCCR with the Kruskal-Wallis test and Spearman correlations (for categorical and
315   continuous variables, respectively). When adequate, statistical significance was adjusted with a
316   Bonferroni correction for multiple testing. We also calculated Cliff's δ statistic (Cliff, 1996) to
317   estimate effect sizes.
318

Results

320

321

322 Data on sociodemographic and clinical characteristics of study participants are displayed in
323 Table 1. Due to the consecutive recruitment strategy, the groups differed in age (H=13.38,
324 p=0.001, degrees of freedom (df)=2), with the aMCI group showing the highest mean age, while
325 the MDD group did not differ from HCs. Also, we found a significant negative correlation
326 between the right LCCR and age (r_s=-0.218, p=0.04). In any case, as described above, all
327 analyses were controlled for age and sex.

328

329 The Kruskal-Wallis test showed significant across-group (MDD n=37, aMCI n=21, HCs n=31)
330 differences in *sra*LCCR (H=16.64, df=2, p=0.001). In post-hoc analyses, it was observed that
331 MDD subjects displayed a lower *sra*LCCR in comparison to aMCI (U=193, Z=-3.16, p<0.005, δ
332 (Cliff's delta effect size) =-0.53) and HCs (U=281, Z=-3.60, p<0.001, δ=-0.51). See Table 3 and
333 Figure 2a. Importantly, our groups did not differ in the signal intensity from the reference region
334 (H=3.47, df=2, p=0.177), and, therefore, *sra*LCCR differences were attributable to differences in
335 LC signal intensity.

336

337 We did not observe any significant effects of aMCI comorbidity in patients with MDD, since no
338 significant differences were found in *sra*LCCR between the subgroup of MDD without aMCI
339 (n=28) and MDD patients with comorbid aMCI (n=9) (U=95, Z=-1.10, p=0.272, δ=−0.25).
340 Likewise, both groups significantly differed from HCs and the aMCI group (see Supplementary
341 Figure S4). Moreover, as depicted in Supplementary Figure S5, we observed no significant
342 correlations between *sra*LCCR values and MMSE scores for any of the study groups.

343

344 When evaluating the possible effects of medication (see Figure 2b), we observed that patients
345 with MDD taking Serotonin and Norepinephrine Reuptake Inhibitors (SNRIs) (n=25) had a
346 significantly lower *sra*LCCR compared to HCs (n=31) (U=143, Z=-4.03, p<0.001, δ=−0.63) and
347 to aMCI patients (n=21) (U=94, Z=-3.72, p<0.001, δ=−0.64). However, we did not observe
348 significant differences in *sra*LCCR between MDD patients taking (n=25) and not taking (n=12)
349 SNRIs, although *sra*LCCR of MDDs patients not taking SNRIs did not differ from HCs (n=31)
350 (U=138, Z=-1.30, p=0.194, δ=−0.26) or aMCI patients (n=21) (U=99, Z=-1.01, p=0.312,
351 δ=−0.21). Although it was not possible to properly evaluate the effect of SNRIs due to the small
352 sample size of the group of MDD subjects exclusively taking SNRIs (n=5), comparing the group
353 of MDD patients taking SNRIs alone with the rest of MDD patients (n=32) and with patients
354 taking SNRIs and other psychiatric medications (n=20) we did not find significant differences
355 (U=60, Z=-0.89, p=0.374, δ=−0.25; and U=43, Z=-0.48, p=0.634, δ=−0.14). Importantly, we did
356 not find any significant differences between MDD patients taking and not taking SNRIs in
357 clinical variables such as severity, disease duration or treatment resistance. These results are
358 presented in Supplementary Table S1.

359

360   Importantly, we repeated the analysis by subdividing the MDD group into those who took (n=31)
361   and those who did not take (n=6) medications with noradrenergic effect (SNRIs + Tricyclics +
362   Mirtazapine + Vortioxetine + Agomelatine + Bupropion), obtaining similar results: MDD taking
363   noradrenergic medication had a significant lower *sra*LCCR compared to HCs (n=31) (U=209,
364   Z=-3.82, p<0.001, δ=−0.57) and the aMCI group (n=21) (U=143, Z=-3.40, p<0.005, δ=−0.56).
365   Again, although we did not observe significant differences in *sra*LCCR between MDD patients
366   taking and not taking noradrenergic medications, *sra*LCCR of MDD patients not taking
367   noradrenergic medications did not differ from HCs (n=31) (U=72, Z=-0.86, p=0.387, δ=−0.23)
368   or aMCI patients (n=21) (U=50, Z=-0.76, p=0.448, δ=−0.21). Also, MDD patients exclusively
369   taking noradrenergic medications other than SNRIs (n=6) did not differ from patients taking
370   SNRIs (n=25), not taking noradrenergic medications (n=6), or the HCs and aMCI groups (see
371   Supplementary Table S2). Finally, we also assessed whether subjects taking adrenergic
372   medication for non-mental health purposes (i.e., beta-blockers; 4 HCs, 1 aMCI and 7 MDD)
373   showed differences in *sra*LCCRs, finding non-significant effects.
374
375   Unfortunately, it was not possible to properly evaluate the effect of Selective Serotonin Reuptake
376   Inhibitors (SSRIs) due to the small sample size of the group of MDD subjects exclusively taking
377   SSRIs (n=3). Nevertheless, comparing the group of MDD patients taking SSRIs alone or in
378   combination with other medications (n=6) with HCs and patients with aMCI, we did not find
379   significant differences after Bonferroni correction (U=32, Z=-2.51, p=0.012, δ=−0.66, and U=20,
380   Z=-2.51, p=0.012, δ=−0.68; Bonferroni p thresholded at p=0.0083).
381
382   Finally, we did not find significant correlations between dose or duration of any of the treatments
383   and *sra*LCCR.
384
385   Unless otherwise indicated, all the above significant findings survived Bonferroni correction for
386   multiple comparisons.
387
388

390 **Discussion**
391
392 Our study compared LC MRI signal intensity between two groups of subjects with brain
393 disorders conferring an increased risk for dementia. We observed that *average*LCCR was
394 significantly lower in late-life MDD patients compared to aMCI and HC groups, but no evidence
395 of additive effects between depression and aMCI. Moreover, such lower LC intensity was
396 associated with the medication used by participants, since significant effects were indeed only
397 observed in the subgroup of MDD patients taking SNRIs.
398
399 Our results are in overall agreement with the monoamine hypothesis of depression (Delgado,
400 2000), which suggests that MDD patients show significant alterations in monoaminergic
401 neurotransmission, and, more specifically, with previous neuroimaging studies reporting a lower
402 LC intensity in patients with MDD compared to HCs (Sasaki et al., 2010; Shibata et al., 2008).
403 Previous reports have shown that NA plays a major role in the pathophysiology of depression
404 (Delgado & Moreno, 2000; Moret, 2011), with the LC projecting to emotion- and cognition-
405 related areas implicated in the pathophysiology of depression (Stahl, 2008).
406
407 In any case, we also observed that this lower LC intensity was specific of MDD patients taking
408 dual action antidepressants (SNRIs). There could be two different explanations for this. On the
409 one hand, if we consider that LC MRI contrast is directly or indirectly associated to the
410 accumulation of neuromelanin compounds (Betts et al., 2019), we could speculate about the
411 nature of such accumulation and the molecular effect of dual antidepressant treatment.
412 Neuromelanin is an autophagic byproduct resulting from the metabolism of NA and other
413 catecholamines (German et al., 1988; Graham, 1979), and its accumulation increases with age in
414 different brain nuclei, such as the substantia nigra and the LC (Clewett et al., 2016). Since SNRIs
415 antidepressants inhibit NA reuptake, the levels of this neurotransmitter are increased at the
416 synaptic cleft, what could lead to a decrease in intracellular NA synthesis and metabolism.
417 Sustained over time, this decrease in NA synthesis and degradation could result in a decreased
418 neuromelanin accumulation in the LC. However, this could have been a strong argument if
419 significant correlations between LC signal intensity and SNRIs treatment dose and duration had
420 been observed, but this was not the case in our study. Moreover, there are no evidences of the
421 existence of an enzymatic mechanism capable of inducing degradation or removing
422 neuromelanin (Fedorow et al., 2006; Halliday et al., 2006), and, therefore, it is not possible to
423 argue that noradrenergic antidepressants may be promoting neuromelanin degradation in LC
424 neurons.
425
426 On the other hand, the possibility exists that particular clinical features of the subgroup of MDD
427 subjects who are taking SNRIs might be associated with the lower LCCR in this group of
428 patients. In our sample, MDD patients taking SNRIs did previously fail to respond to treatments
429 with SSRIs. Speculatively, this treatment failure could be related to an impaired NA function

430   reflected in lower MRI LCCR that required the active modulation of NA neurotransmission.
431   Although treatment with dual action antidepressant does not seem to normalize LCCR intensity
432   levels, prospective research on the interaction between antidepressant medication with
433   noradrenergic action and LC signal intensity, carefully controlling for doses and treatment
434   duration, is warranted to elucidate this issue.
435
436   Contrary to our initial expectations, we did not observe any significant effect of aMCI on LC
437   signal intensities, which prevents suggesting LC MRI intensity as a putative risk imaging marker
438   for AD. These results contradict previous research showing not only an early loss of LC neurons
439   in AD (Szot et al, 2006), but also lower LC intensity values in aMCI versus HCs (Takahashi et
440   al, 2015). Critically, however, that study did not exclude patients with comorbid depression,
441   while our group of aMCI individuals did not show comorbidity with major depression.
442   Therefore, we propose that MDD symptoms may be actually more relevantly accounting for
443   lower LC signal intensity. In agreement with this, we have also observed that the presence of
444   comorbid aMCI in patients with MDD did not significantly contribute to further lowering LC
445   signal intensities.
446
447   This study is not without limitations. First, since we did not obtain data on cerebrospinal fluid or
448   PET imaging biomarkers, we used a syndromic categorical cognitive staging approach and we
449   cannot confirm that our patients were indeed from the AD continuum and will ultimately develop
450   AD. Second, longitudinal studies with larger and carefully characterized samples are highly
451   encouraged in order to better explore the interactions over time of group findings with clinical
452   and sociodemographic variables. This will probably allow identifying clinically relevant
453   subgroups of individuals as a function of their LC signal intensities and contribute to better
454   estimate the likelihood of a degenerative course. Third, we are not using a quantitative MRI
455   method, although other MRI sequences, such as Magnetization Transfer (MT), may provide
456   quantitative indices (Ramani et al., 2002; Sled and Pike, 2001) that have been used for assessing
457   LC integrity (Trujillo et al., 2019). As many other groups, we used a Spin Echo (SE) sequence
458   for assessing LC neuronal integrity (Liu et al., 2017), although MT based sequences seem to be a
459   better option to perform absolute signal quantifications (Trujillo et al., 2019) and to more
460   precisely localize the LC with isotropic resolution and increased contrast-to-noise ratio,
461   especially at higher-field strengths (Priovoulos et al., 2018). We performed a relative
462   quantification taking another brainstem region as the reference area to control for intensity
463   fluctuations across participants, and, importantly, groups did not significantly differ in the
464   intensity of this reference region, indicating that our group differences stem from differences in
465   LC intensity. Nevertheless, further studies combining quantitative and non-quantitative
466   approaches are probably needed to perform better estimations of neural integrity in the LC (Betts
467   et al., 2019). Likewise, the present approach did not allow quantifying the volume of the LC,
468   which would have required performing a manual segmentation of the nucleus, and, therefore, we
469   can only infer changes in LC integrity from changes in MRI signal intensity. If such signal

470   intensity is related to neuromelanin accumulation, LC integrity will be probably
471   reflectingpreserved adrenergic activity. By contrast, if such signal is related to higher neuronal
472   density or water content, as recently suggested (Watanabe et al., 2019), LC integrity will be
473   reflecting a lack of regional atrophy and/or a good osmotic balance in the context of a normal
474   neuronal metabolism.
475
476   In the context of limitations, it is also important to note that there are studies suggesting that age-
477   related variance should be considered when exploring structural abnormalities in the LC (Shibata
478   et al, 2006; Liu et al., 2019). Moreover, these age effects may probably show a non-homogenous
479   distribution along the rostral-caudal axis of the nucleus (Betts et al, 2017; Dahl et al., 2019; Liu
480   et al., 2019). Thus, age-related declines in LCCR have been mainly observed in the rostral part of
481   the LC in healthy subjects (Liu et al., 2019), being such decline in rostral LCCRs related to
482   poorer memory performance in neuropsychological testing (Dahl et al., 2019). Although we
483   controlled for age and sex, our algorithm did not allow distinguishing between the rostral and the
484   caudal parts of the nucleus, which may have partially confounded our findings. Moreover, white
485   matter from the pontine tegmentum, used here as reference, has also been shown to increase its
486   T1 intensity with age, probably as a consequence of the highly protracted cycle of myelination of
487   this region, extending up to 70 or 80 years of age (Yakolev and Lecours, 1967). Despite our
488   statistical control for age, and although our groups did not differ in the signal intensity of this
489   reference region, this may have also partially confounded our findings.
490
491

492   **Conclusions**
493
494   To sum up, LC signal intensity does not seem to allow identifying subjects with cognitive
495   profiles related to prodromal phases of AD. Conversely, it seems to be associated to late-life
496   MDD. Further research with larger samples should ascertain whether medication aimed at
497   modulating noradrenergic neurotransmission may be playing a role in these findings or,
498   conversely, changes in LC neurons are associated with a particular clinical profile preferentially
499   observed in patients responding to noradrenergic medication. It also remains to be determined if
500   these findings may contribute to optimizing treatment of patients with late-life MDD.
501
502

503   **Acknowledgements**
504

505   The authors are grateful to all the study participants and their families, and to the staff and
506   technicians of Bellvitge University Hospital and Duran i Reynals Hospital who helped to recruit
507   the sample for this study. We thank CERCA Programme/Generalitat de Catalunya for
508   institutional support.
509

510

Author Contributions

512

513 Conceptualization, I.F., J.M.M., V.S. and C.S-M.; Methodology, A.G-I., I.M-Z., I.dC., G.B. and
514 C.S-M.; Software, I.M-Z. and P.C.; Validation, A.G-I., I.M-Z. and C.S-M.; Formal Analysis,
515 A.G-I., M.G. and I.M-Z.; Investigation, A.G-I., I.dC., J.G., R.R., I.R., A.C., M.U. and V.S.;
516 Resources, C.A., I.F., J.M.M. and C.S-M.; Data Curation, J.G., R.R., I.R., A.C., C.A., M.U.,
517 V.S., J.M.M. and C.S-M.; Writing – Original Draft Preparation, A.G-I., M.G. and C.S-M.;
518 Writing – Review & Editing, All authors; Visualization, A.G-I., M.G., I.dC. and C.S-M.;
519 Supervision, C.S-M; Project Administration, V.S. and C.S-M.; Funding Acquisition, I.F., J.M.M.
520 and C.S-M.

521
522

Conflicts of Interest

524

525 The authors report no biomedical financial interests or potential conflicts of interest regarding
526 this work.

527

528 Dr. Soria has received grants and served as a consultant or continuing medical education (CME)
529 speaker for Lundbeck, Otsuka, Janssen-Cilag, Exeltis and the Institute of Health Carlos III
530 through the Spanish Ministry of Economy and Competitiveness. Dr. Urretavizcaya has been
531 funded by the Institute of Health Carlos III through the Spanish Ministry of Economy and
532 Competitiveness and has received compensation for lectures, advisories, or grants from Janssen-
533 Cilagand Lundbeck. Dr. Menchón has received grants and served as a consultant, advisor or
534 CME speaker for Janssen-Cilag, Lundbeck, Medtronic, Otsuka, and the Spanish Ministry of
535 Economy and Competitiveness (CIBERSAM).

536

537 The rest of authors have nothing to disclose nor have any financial relationships with commercial
538 interests.

References

Alegret, M.; Espinosa, A.; Vinyes-Junqué, G.; Valero, S.; Hernández, I.; Tárraga, L.; Becker, J.T.; Boada, M. Normative data of a brief neuropsychological battery for Spanish individuals older than 49. *J Clin Exp Neuropsychol* **2012**, *34*, 209–219.

Andrés-Benito, P.; Fernández-Dueñas, V.; Carmona, M.; Escobar, L.A.; Torrejón-Escribano, B.; Aso, E; Ciruela, F; Ferrer I. Locus coeruleus at asymptomatic early and middle Braak stages of neurofibrillary tangle pathology. *Neuropathol Appl Neurobiol* **2017**, *43*, 373–392.

Bangasser, D. A., Wiersielis, K. R., & Khantsis, S. Sex Differences in the Locus Coeruleus-Norepinephrine System and its Regulation by Stress. *Brain Research* **2016**, 1641 *(PtB)*, 177–188.

Berridge, C.W.; Waterhouse, B.D. The locus coeruleus-noradrenergic system: modulation of behavioral state and state-dependent cognitive processes. *Brain Res. Brain Res. Rev.* **2003**, *42*, 33–84.

Betts, M.J.; Cardenas-Blanco, A.; Kanowski, M.; Jessen, F.; Düzel, E. In vivo MRI assessment of the human locus coeruleus along its rostrocaudal extent in young and older adults. *Neuroimage* **2017**, *163*, 150–159.

Betts, M.J.; Kirilina, E.; Otaduy, M.C.G.; Ivanov, D.; Acosta-Cabronero, J.; Callaghan, M.F.; Lambert, C.; Cardenas-Blanco, A.; Pine, K.; Passamonti, L.; Loane, C.; Keuken, M.C.; Trujillo, P.; Lüsebrink, F.; Mattern, H.; Liu, K.Y.; Priovoulos, N.; Fliessbach, K.; Dahl, M.J.; Maaß, A.; Madelung, C.F.; Meder, D.; Ehrenberg, A.J.; Speck, O.; Weiskopf, N.; Dolan, R.; Inglis, B.; Tosun, D.; Morawski, M.; Zucca, F.A.; Siebner, H.R.; Mather, M.; Uludag, K.; Heinsen, H.; Poser, B.A.; Howard, R.; Zecca, L.; Rowe, J.B.; Grinberg, L.T.; Jacobs, H.I.L.; Düzel, E.; Hämmerer, D. Locus coeruleus imaging as a biomarker for noradrenergic dysfunction in neurodegenerative diseases. *Brain* **2019**, *142*, 2558–2571.

Braak, H.; Del Tredici, K. The preclinical phase of the pathological process underlying sporadic Alzheimer's disease. *Brain* **2015**, *138*, 2814–2833.

Braak, H.; Thal, D.R.; Ghebremedhin, E.; Del Tredici, K. Stages of the pathologic process in alzheimer disease: Age categories from 1 to 100 years. *J Neuropathol Exp Neurol* **2011**, *70*, 960–969.

Byers, A.L.; Yaffe, K. Depression and risk of developing dementia. *Nat Rev Neurol* **2011**, *7*, 323–331.

Charney, D.S. Monoamine dysfunction and the pathophysiology and treatment of depression. *J Clin Psychiatry* **1998**, *59 Suppl 14*, 11–14.

580 Clewett, D.V.; Lee, T.-H.; Greening, S.; Ponzio, A.; Margalit, E.; Mather, M. Neuromelanin
581 marks the spot: identifying a locus coeruleus biomarker of cognitive reserve in healthy aging.
582 *Neurobiol. Aging* **2016**, *37*, 117–126.

583 Cliff, N. Answering Ordinal Questions with Ordinal Data Using Ordinal Statistics. Multivariate
584 *Behav Res* **1996**, *31*, 331–350.

585 Dahl, M.J.; Mather, M.; Düzel, S.; Bodammer, N.C.; Lindenbergr, U.; Kühn, S.; Werkle-
586 Bergner, M. Rostral locus Coeruleus integrity is associated with better memory performance in
587 older adults. *Nature Human Behaviour* **2019**, *3*, 1203-1214.

588 Dahlstroem, A.; Fuxe, K. Evidence for the existence of monoamine-containing neurons in the
589 central nervous system. I. Demonstration of monoamines in the cell bodies of brain stem
590 neurons. *Acta Physiol Scand Suppl* **1964**, *Suppl 232*, 1-55.

591 Delgado, P.L.; Moreno, F.A. Role of norepinephrine in depression. *J Clin Psychiatry* **2000**, *61
592 Suppl 1*, 5–12.

593 Delgado, P.L. Depression: the case for a monoamine deficiency. *J Clin Psychiatry* **2000**, *61
594 Suppl 6*, 7–11.

595 Enochs, W.S.; Hyslop, W.B.; Bennett, H.F.; Brown, R.D.; Koenig, S.H.; Swartz, H.M. Sources
596 of the increased longitudinal relaxation rates observed in melanotic melanoma. An in vitro study
597 of synthetic melanins. *Investigative Radiology* **1989**, *24*, 794—804.

598 Enochs, W.S.; Petherick, P.; Bogdanova, A.; Mohr, U.; Weissleder, R. Paramagnetic metal
599 scavenging by melanin: MR imaging. *Radiology* **1997**, *204*, 417–423.

600 Fedorow, H.; Halliday, G.M.; Rickert, C.H.; Gerlach, M.; Riederer, P.; Double, K.L. Evidence
601 for specific phases in the development of human neuromelanin. *Neurobiol. Aging* **2006**, *27*, 506–
602 512.

603 Folstein, M.F.; Folstein, S.E.; McHugh, P.R. "Mini-mental state". A practical method for grading
604 the cognitive state of patients for the clinician. *J Psychiatr Res* **1975**, *12*, 189–198.

605 Gabryelewicz, T.; Styczynska, M.; Luczywek, E.; Barczak, A.; Pfeffer, A.; Androsiuk, W.;
606 Chodakowska-Zebrowska, M.; Wasiak, B.; Peplonska, B.; Barcikowska, M. The rate of
607 conversion of mild cognitive impairment to dementia: predictive role of depression. *Int J Geriatr
608 Psychiatry*. **2007**;*22*:563–567.

609 Gannon, M.; Che, P.; Chen, Y.; Jiao, K.; Roberson, E.D.; Wang, Q. Noradrenergic dysfunction
610 in Alzheimer's disease. *Front Neurosci* **2015**, *9*, 220.

611 García-Lorenzo, D.; Longo-Dos Santos, C.; Ewencyk, C.; Leu-Semenescu, S.; Gallea, C.;
612 Quattrocchi, G; Pita Lobo, P.; Poupon, C.; Benali, H.; Arnulf, I; Vidailhet, M.; Lehericy, S. The
613 Coeruleus/subcoeruleus complex in rapid eye movement sleep behavior disorders in Parkinson's
614 disease. *Neuroimage* **2013**, *136*, 2120–2129.

615   German, D.C.; Walker, B.S.; Manaye, K.; Smith, W.K.; Woodward, D.J.; North, A.J. The human
616   locus coeruleus: computer reconstruction of cellular distribution. *J. Neurosci.* **1988**, *8*, 1776–
617   1788.

618   Graham, D.G. On the origin and significance of neuromelanin. *Arch. Pathol. Lab. Med.* **1979**,
619   *103*, 359–362.

620   Grudzien, A.; Shaw, P.; Weintraub, S.; Bigio, E.; Mash, D.C.; Mesulam, M.M. Locus coeruleus
621   neurofibrillary degeneration in aging, mild cognitive impairment and early Alzheimer's disease.
622   *Neurobiol Aging* **2007**, *28*, 327-335.

623   Halliday, G.M.; Fedorow, H.; Rickert, C.H.; Gerlach, M.; Riederer, P.; Double, K.L. Evidence
624   for specific phases in the development of human neuromelanin. *J Neural Transm (Vienna)* **2006**,
625   *113*, 721–728.

626   Hamilton, M. A rating scale for depression. *J. Neurol. Neurosurg. Psychiatry* **1960**, *23*, 56–62.

627   Heneka, M.T.; Ramanathan, M.; Jacobs, A.H.; Dumitrescu-Ozimek, L.; Bilkei-Gorzo, A.;
628   Debeir, T.; Sastre, M.; Galldiks, N.; Zimmer, A.; Hoehn, M.; Heiss, W-D.; Klockgether T.;
629   Staufenbiel, M. Locus Coeruleus Degeneration Promotes Alzheimer Pathogenesis in Amyloid
630   Precursor Protein 23 Transgenic Mice. *J Neurosci* **2006**, *26*, 1343-1354.

631   Hermida, A.P.; McDonald, W.M.; Steenland, K.; Levey, A. The association between late-life
632   depression, mild cognitive impairment and dementia: is inflammation the missing link? *Expert*
633   *Rev Neurother* **2012**, *12*, 1339–1350.

634   Isaias, I.U.; Trujillo, P.; Summers, P.; Marotta, G.; Mainardi, L.; Pezzoli, G.; Zecca, L.; Costa,
635   A. Neuromelanin Imaging and Dopaminergic Loss in Parkinson's Disease. *Front Aging Neurosci*
636   **2016**, *8*, 196.

637   Jack, C.R.; Bennett, D.A.; Blennow, K.; Carrillo, M.C.; Dunn, B.; Budd Haeberlein, S.;
638   Holtzman, D.M.; Jagust, W.; Jessen, F.; Karlawish, J.; Liu, E.; Molinuevo, J.L.; Montine, T.;
639   Phelps, C.; Rankin, K.P.; Rowe, C.C.; Scheltens, P.; Siemers, E.; Snyder, H.M.; Sperling, R.;
640   Collaborators. NIA-AA Research Framework: Toward a biological definition of Alzheimer's
641   disease. *Alzheimer's Dement* **2018**, *14*, 535–562.

642   Keren, N.I.; Taheri, S.; Vazey, E.M.; Morgan, P.S.; Granholm, A.-C.E.; Aston-Jones, G.S.;
643   Eckert, M.A. Histologic validation of locus coeruleus MRI contrast in post-mortem tissue.
644   *NeuroImage* **2015**, *113*, 235–245.

645   Leonard, B.E. The role of noradrenaline in depression: a review. *J. Psychopharmacol. (Oxford)*
646   **1997**, *11*, S39-47.

647   Liu, K.Y.; Marijatta, F.; Hämmerer, D.; Acosta-Cabronero, J.; Düzel, E.; Howard, R.J. Magnetic
648   resonance imaging of the human locus coeruleus: A systematic review. *Neurosci Biobehav Rev*
649   **2017**, *83*, 325–355.

650   Liu, K.Y.; Acosta-Cabronero, J.; Cardenas-Blanco, A.; Loane, C.; Berry, A.J.; Betts, M.J.;
651   Kievit, R.A.; Henson, R.N.; Düel, E.; Cam-CAN; Howard, R.; Hämmerer, D. In vivo

652 visualization of age-related differences in the locus coeruleus. *Neurobiol Aging* **2019**, *74*, 101-
653 111.

654 Lobo, A., Saz, P., Marcos, G., Día, J.L., de la Cámara, C., Ventura, T., Morales Asín, F.,
655 Pascual, F.L., Montañés, J.A., Aznar, S. Revalidación y normalización del miniexamen
656 cognoscitivo (primera versión en castellano del Minimental State Examination) en la población
657 general geriátrica. *Med Clin (Barc)* **1999,** *112*, 767-774.

658

659 Loughlin, S.E.; Foote, S.L.; Fallon, J.H. Locus coeruleus projections to cortex: topography,
660 morphology and collateralization. *Brain Res. Bull.* **1982**, *9*, 287–294.

661

662 Loughlin, S.E.; Foote, S.L.; Bloom, F.E. Efferent projections of nucleus locus coeruleus:
663 topographic organization of cells of origin demonstrated by three-dimensional reconstruction.
664 *Neuroscience* **1986**, *18*, 291–306.

665

666 Loughlin, S.E.; Foote, S.L.; Grzanna, R. Efferent projections of nucleus locus coeruleus:
667 morphologic subpopulations have different efferent targets. *Neuroscience* **1986**, *18*, 307–319.

668

669 Marien, M.R.; Colpaert, F.C.; Rosenquist, A.C. Noradrenergic mechanisms in neurodegenerative
670 diseases: A theory. *Brain Res Rev* **2004**, *45*, 38-78.

671

672 Matsuura, K.; Maeda, M.; Yata, K.; Ichiba, Y.; Yamaguchi, T.; Kanamaru, K.; Tomimoto, H.
673 Neuromelanin magnetic resonance imaging in Parkinson's disease and multiple system atrophy.
674 *Eur. Neurol.* **2013**, *70*, 70–77.

675

676 Miyoshi, F.; Ogawa, T.; Kitao, S. -i; Kitayama, M.; Shinohara, Y.; Takasugi, M.; Fujii, S.;
677 Kaminou, T. Evaluation of Parkinson disease and Alzheimer disease with the use of
678 neuromelanin MR imaging and (123)I-metaiodobenzylguanidine scintigraphy. *AJNR Am J*
679 *Neuroradiol* **2013**, *34*, 2113–2118.

680 Modrego, P.J.; Ferrandez, J. Depression in patients with mild cognitive impairment increases the
681 risk of developing dementia of Alzheimer type: a prospective cohort study. *Arch Neurol* **2004**,
682 *61*, 1290–1293.

683 Moret, C.; Briley, M. The importance of norepinephrine in depression. *Neuropsychiatr Dis Treat*
684 **2011**, *7*, 9–13.

685 Morris, J.C. The Clinical Dementia Rating (CDR): current version and scoring rules. *Neurology*
686 **1993**, *43*, 2412–2414.

687 Mukai, M.; Sugaya, K.; Yabe, I.; Goto, Y.; Yokochi, F.; Miyamoto, K.; Cai, H.; Sasaki, H.;
688 Matsubara, S. Neuromelanin MRI in a family with mitochondrial parkinsonism harboring a
689 Y955C mutation in POLG1. *Parkinsonism Relat. Disord.* **2013**, *19*, 821–824.

690 Mulvey, B.; Bhatti, D.L.; Gyawali, S.; Lake, A. M.; Kriaucionis, S.; Ford, C.P.; Bruchas, M.R.;
691 Heintz, N.; Dougherty, J.D. Molecular and Functional Sex Differences of Noradrenergic
692 Neurons in the Mouse Locus Coeruleus. *Cell Reports* **2018**, 23, 2225–2235.
693

694 Ohtsuka, C.; Sasaki, M.; Konno, K.; Kato, K.; Takahashi, J.; Yamashita, F.; Terayama, Y.
695 Differentiation of early-stage parkinsonisms using neuromelanin-sensitive magnetic resonance
696 imaging. *Parkinsonism Relat. Disord.* **2014**, *20*, 755–760.

697 Panza, F.; Frisardi, V.; Capurso, C.; D'Introno, A.; Colacicco, A. M.; Imbimbo, B. P.; Santamato,
698 A.; Vendemiale, G.; Seripa, D.; Pilotto, A.; Capurso, A.; Solfrizzi, V. Late-life depression, mild
699 cognitive impairment, and dementia: possible continuum?. *The Am J Geriatr Psychiatry* **2010**,
700 *18*, 98–116.

701 Petersen, R.C. Mild cognitive impairment as a diagnostic entity. *J. Intern. Med.* **2004**, *256*, 183–
702 194.

703 Petersen, R.C.; Doody, R.; Kurz, A.; Mohs, R.C.; Morris, J.C.; Rabins, P.V.; Ritchie, K.; Rossor,
704 M.; Thal, L.; Winblad, B. Current concepts in mild cognitive impairment. *Arch. Neurol.* **2001**,
705 *58*, 1985–1992.

706 Priovoulos, N.; Jacobs, H.; Ivanov, D.; Uludağ, K.; Verhey, F.; Poser, B. A. High-resolution in
707 vivo imaging of human locus coeruleus by magnetization transfer MRI at 3T and
708 7T. *NeuroImage* **2018**, *168*, 427–436.

709 Ramani, A.; Dalton, C.; Miller, D.H.; Tofts, P.S.; Barker, G.J. Precise estimate of fundamental
710 in-vivo MT parameters in human brain in clinically feasible times. *Magn Reson Imaging* **2002**,
711 *20*, 721–731.

712 Samuels, E.R.; Szabadi, E. Functional neuroanatomy of the noradrenergic locus coeruleus: its
713 roles in the regulation of arousal and autonomic function part I: principles of functional
714 organisation. *Curr Neuropharmacol* **2008**, *6*, 235–253.

715 Sasaki, M.; Shibata, E.; Ohtsuka, K.; Endoh, J.; Kudo, K.; Narumi, S.; Sakai, A. Visual
716 discrimination among patients with depression and schizophrenia and healthy individuals using
717 semiquantitative color-coded fast spin-echo T1-weighted magnetic resonance imaging.
718 *Neuroradiology* **2010**, *52*, 83–89.

719 Sasaki, M.; Shibata, E.; Tohyama, K.; Takahashi, J.; Otsuka, K.; Tsuchiya, K.; Takahashi, S.;
720 Ehara, S.; Terayama, Y.; Sakai, A. Neuromelanin magnetic resonance imaging of locus
721 coeruleus and substantia nigra in Parkinson's disease. *Neuroreport* **2006**, *17*, 1215–1218

722 Sheehan, D.V.; Lecrubier, Y.; Sheehan, K.H.; Amorim, P.; Janavs, J.; Weiller, E.; Hergueta, T.;
723 Baker, R.; Dunbar, G.C. The Mini-International Neuropsychiatric Interview (M.I.N.I.): the
724 development and validation of a structured diagnostic psychiatric interview for DSM-IV and
725 ICD-10. *J Clin Psychiatry* **1998**, *59 Suppl 20*, 22-33;quiz 34-57.

726   Sheikh, J.I.; Yesavage, J.A. Geriatric Depression Scale (GDS): Recent evidence and
727   development of a shorter version. *Clinical Gerontologist: The Journal of Aging and Mental*
728   *Health* **1986**, *5*, 165–173.

729   Shibata, E.; Sasaki, M.; Tohyama, K.; Kanbara, Y.; Otsuka, K.; Ehara, S.; Sakai, A. Age-related
730   changes in locus ceruleus on neuromelanin magnetic resonance imaging at 3 Tesla. *Magn Reson*
731   *Med Sci* **2006**, *5*, 197–200.

732   Shibata, E.; Sasaki, M.; Tohyama, K.; Otsuka, K.; Endoh, J.; Terayama, Y.; Sakai, A. Use of
733   neuromelanin-sensitive MRI to distinguish schizophrenic and depressive patients and healthy
734   individuals based on signal alterations in the substantia nigra and locus ceruleus. *Biol. Psychiatry*
735   **2008**, *64*, 401–406.

736   Shima, T.; Sarna, T.; Swartz, H.M.; Stroppolo, A.; Gerbasi, R.; Zecca, L. Binding of iron to
737   neuromelanin of human substantia nigra and synthetic melanin: an electron paramagnetic
738   resonance spectroscopy study. *Free Radic Biol Med* **1997**, *23*, 110–119.

739   Sled, J.G.; Pike, G.B. Quantitative imaging of magnetization transfer exchange and relaxation
740   properties in vivo using MRI. *Magn Reson Med* **2001**, *46*, 923–931.
741
742   Stahl, S.M. *Stahl's essential psychopharmacology: Neuroscientific basis and practical*
743   *applications, 3rd ed*; Stahl's essential psychopharmacology: Neuroscientific basis and practical
744   applications, 3rd ed; Cambridge University Press: New York, NY, US, 2008.

745   Steffens, D.C. Depressive symptoms and mild cognitive impairment in the elderly: an ominous
746   combination. *Biol Psychiatry* **2012**, *71*, 762–764.

747   Szot, P.; White, S.S.; Greenup, J.L.; Leverenz, J.B.; Peskind, E.R.; Raskind, M.A. Compensatory
748   changes in the noradrenergic nervous system in the locus ceruleus and hippocampus of
749   postmortem subjects with Alzheimer's disease and dementia with Lewy bodies. *J. Neurosci.*
750   **2006**, *26*, 467–478.

751   Takahashi, J.; Shibata, T.; Sasaki, M.; Kudo, M.; Yanezawa, H.; Obara, S.; Kudo, K.; Ito, K.;
752   Yamashita, F.; Terayama, Y. Detection of changes in the locus coeruleus in patients with mild
753   cognitive impairment and Alzheimer's disease: High-resolution fast spin-echo T1-weighted
754   imaging. *Geriatr Gerontol Int* **2015**, *15*, 334–340.

755   Tosk, J.M.; Holshouser, B.A.; Aloia, R.C.; Hinshaw, D.B.; Hasso, A.N.; MacMurray, J.P.; Will,
756   A.D.; Bozzetti, L.P. Effects of the interaction between ferric iron and L-dopa melanin on T1 and
757   T2 relaxation times determined by magnetic resonance imaging. *Magn Reson Med* **1992**, *26*, 40–
758   45.

759   Trujillo, P.; Summers, P.E.; Ferrari, E.; Zucca, F.A.; Sturini, M.; Mainardi, L.T.; Cerutti, S.;
760   Smith, A.K.; Smith, S.A.; Zecca, L.; Costa, A. Contrast mechanisms associated with
761   neuromelanin-MRI. *Magn Reson Med* **2017**, *78*, 1790–1800.

762 Trujillo, P.; Petersen, K.J.; Cronin, M.J.; Lin, Y.C.; Kang, H.; Donahue, M.J.; Smith, S.A.;
763 Claassen, D.O. Quantitative magnetization transfer imaging of the human locus coeruleus.
764 *Neuroimage* **2019**, *15*, 191-198.

765 Watanabe, T.; Tan, Z.; Wang, X.; Martinez-Hernandez, A.; Frahm, J. Magnetic resonance
766 imaging of noradrenergic neurons. *Brain Struct Funct* **2019**, *224*, 1609-1625.

767 Wechsler, D. *Escala de inteligencia de Wechsler para adultos-III*; TEA Ediciones: Madrid,
768 Spain, **1999**.

769 Wechsler, D. *WMS-III. Escala de Memoria Wechsler - III*; TEA Ediciones: Madrid, Spain, **2004**.

770 Yakovlev, P.I.; Lecours, A.R. The myelogenetic cycles of regional maturation of the brain.
771 Regional Development of the Brain in Early Life A. Blackwell Scientific: Oxford, **1967**.

772 Yesavage, J.A.; Brink, T.L.; Rose, T.L.; Lum, O.; Huang, V.; Adey, M.; Leirer, V.O.
773 Development and validation of a geriatric depression screening scale: a preliminary report. *J*
774 *Psychiatr Res* **1982**, *17*, 37–49.

775 Zarow, C.; Lyness, S.A.; Mortimer, J.A.; Chui, H.C. Neuronal loss is greater in the locus
776 coeruleus than nucleus basalis and substantia nigra in Alzheimer and Parkinson diseases. *Arch*
777 *Neurol* **2003**, *60*, 337–341.

Characteristics of the study sample.

Abbreviations: aMCI, amnestic Mild Cognitive Impairment; df, degrees of freedom; GDS, Geriatric Depression Scale; HDRS, Hamilton Depression Rating Scale; MDD, late-life Major Depression Disorder; MMSE, Mini-Mental State Examination; SD, Standard Deviation. [a]Statistic value corresponds to Kruskal-Wallis H test for continuous variables and Chi-Square test for categorical variables.

[b]The cut-off in the Spanish version of the MMSE (Lobo et al., 1999) is adjusted for age and schooling years. Scores higher than 23 for literate people and higher than 18 for illiterates indicate preserved general cognitive functioning.

[c] Evaluated with the delayed recall test from the Wechsler Memory Scale III (WMS-III).

1   **Table 1**. Characteristics of the study sample.

	MDD patients n=37	aMCI patients n= 21	Controls n=31	Statistic (p value)[a] df
Sociodemographic characteristics				
Age, years; mean (SD) [range]	68 (4.1) [60-74]	71.5 (2.7) [67-76]	67.7 (4.1) [60-75]	H=1.38 (0.001) 2
Sex, male; n (%)	11 (29.7)	9 (42.9)	11 (35.5)	X^2=1.03 (0.599) 2
Clinical characteristics				
HDRS; mean (SD) [range]	12.1 (7.1) [1-28]	3.8 (3) [0-8]	1.3 (2.8) [0-15]	H=50.85 (<0.0001) 2
GDS; mean (SD) [range]	5.6 (4.3) [0-13]	2.3 (2.2) [0-9]	1.23 (2.3) [0-12]	H=27.7 (<0.0001) 2
MMSE; mean (SD) [range][b]	25.9 (3.3) [13-30]	25.8 (2.6) [20-29]	28.9 (1.49) [24-30]	H=32.68 (<0.0001) 2
Long Term Memory [c]; (SD) [range]	5.08 (2.54) [0-10]	1.95 (1.28) [0-4]	8.32 (1.72) [6-12]	H=53.93 (<0.0001)

				2

Abbreviations: aMCI, amnestic Mild Cognitive Impairment; df, degrees of freedom; GDS, Geriatric Depression Scale; HDRS, Hamilton Depression Rating Scale; MDD, late-life Major Depression Disorder; MMSE, Mini-Mental State Examination; SD, Standard Deviation.

[a] Statistic value corresponds to Kruskal-Wallis H test for continuous variables and Chi-Square test for categorical variables.

[b] The cut-off in the Spanish version of the MMSE (Lobo et al., 1999) is adjusted for age and schooling years. Scores higher than 23 for literate people and higher than 18 for illiterates indicate preserved general cognitive functioning.

[c] Evaluated with the delayed recall test from the Wechsler Memory Scale III (WMS-III).

Antidepressant treatment at the time of the study

Abbreviations: aMCI, amnestic Mild Cognitive Impairment; MDD, late-life Major Depression Disorder; SD, Standard Deviation.

1 **Table 2**. Antidepressant treatment at the time of the study.

n (%) [dose-range in mg]	
MDD patients n=37	**aMCI patients n=21**
Tricyclics	

	MDD patients n=37	**aMCI patients n=21**
Tricyclics		
Clomipramine	2 (5.4) [37.5-75]	0 (0) [0]
Imipramine	2 (5.4) [75-175]	0 (0) [0]
Amitriptyline	1 (2.7) [25]	2 (9.5) [20-25]
Selective serotonin reuptake inhibitors (SSRIs)		
Sertraline	1 (2.7) [200]	0 (0) [0]
Citalopram	2 (5.4) [10]	4 (19.1) [10-20]
Paroxetine	3 (8.1) [20-30]	0 (0) [0]
Serotonin–norepinephrine reuptake inhibitor (SNRIs)		
Venlafaxine	12 (32.4) [75-300]	0 (0) [0]
Duloxetine	11 (29.7) [60-120]	0 (0) [0]
Desvenlafaxine	2 (5.4) [50-100]	0 (0) [0]
Other antidepressants		
Mirtazapine	7 (18.9) [15-30]	2 (9.5) [7.5-15]
Bupropion	5 (13.5) [150-300]	0 (0) [0]
Vortioxetine	1 (2.7) [10]	0 (0) [0]
Agomelatine	2 (5.4) [25]	0 (0) [0]
Trazodone	4 (10.8) [50-100]	7 (33.3) [50-100]

4 Abbreviations: aMCI, amnestic Mild Cognitive Impairment; MDD, late-life Major Depression
5 Disorder; SD, Standard Deviation.

Average LC Contrast Ratios.

Abbreviations: aMCI, amnestic Mild Cognitive Impairment; HCs, Healthy Controls; LC: Locus Coeruleus; MDD, late-life Major Depressive Disorder; SD, Standard Deviation; SNRIs, Serotonin and Norepinephrine reuptake inhibitors.

1   **Table 3**. Average LC Contrast Ratios.

	Average LC Contrast Ratio Intensity: mean (SD)	Standardized residual of Average LC Contrast Ratio *(sra*LCCR) Intensity: mean (SD)
MDD whole group (n=37)	0.194 (0.059)	-0.450 (0.0728)
MDD with aMCI (n=9)	0.195 (0.084	-0.474 (1.016)
MDD without aMCI (n=28)	0.194 (0.052)	-0.442 (0.633)
aMCI (n= 21)	0.234 (0.079)	0.257 (0.946)
HCs (n=31)	0.260 (0.093)	0.363 (1.096)
MDD split according to SNRIs treatment		
MDD taking SNRIs (n=25)	0.180 (0.045)	-0.621 (0.538)
MDD not taking SNRIs (n=12)	0.224 (0.076)	-0.094 (0.947)

3   Abbreviations: aMCI, amnestic Mild Cognitive Impairment; HCs, Healthy Controls; LC: Locus
4   Coeruleus; MDD, late-life Major Depressive Disorder; SD, Standard Deviation; SNRIs,
5   Serotonin and Norepinephrine reuptake inhibitors.

Figure 1

Visualization and localization of the LC and the reference region

Figure 1. **a):** Axial, coronal and sagittal views of the dorsal pons from the modified fast spin-echo T1 sequence of a representative participant (see text for details). The LC can be identified in each hemisphere as an hyperintense structure (red arrows). **b):** Axial, coronal and sagittal views of the dorsal pons from the high-dimensional whole-brain T1 sequence of the same participant, depicting, in red, the 10 most intense LC voxels as identified by the growing algorithm. The denormalized ROI of the LC and reference regions are depicted as red (encompassing the 10 most intense LC voxels) and blue contours, respectively.
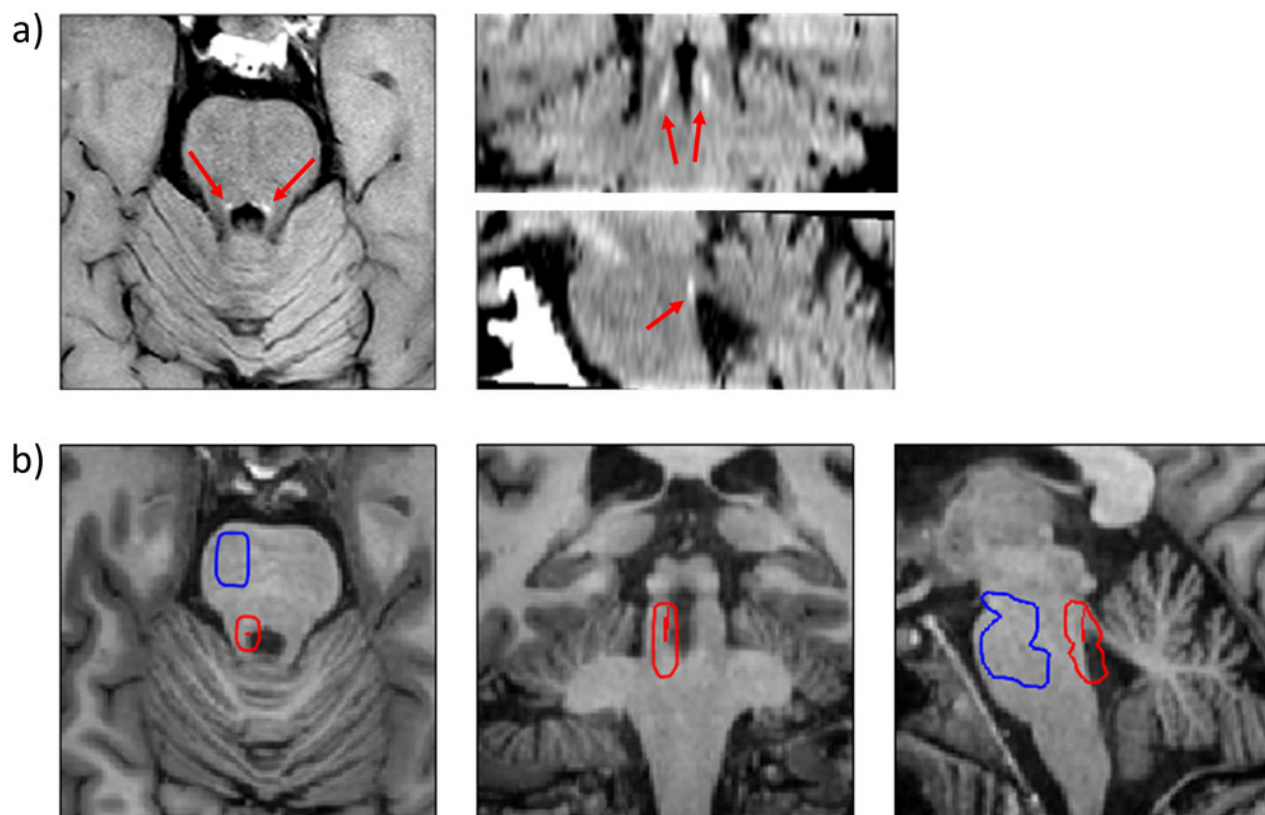
Figure 2

Boxplots depicting the average LC Contrast Ratios

Figure 2. Boxplots showing the *average* LCCR (age and sex adjusted, *sra*LCCR) for the different study groups. The individual values (dots) are overlaid for reference. a) Boxplots of the *average LCCR* for the three main study groups; b) Boxplots of the *average* LCCR splitting patients with late-life MDD as a function of SNRIs treatment. aMCI, amnestic type Mild Cognitive Impairment; HCs, Healthy Controls; LCCR, Locus Coeruleus Contrast Ratio; MDD, late-life Major Depressive Disorder. **p≤0.005, ***p≤0.001. All results remained significant after excluding outlier values.